Published in final edited form as:
Free Radic Biol Med. 2010 February 15; 48(4): 493–498. doi:10.1016/j.freeradbiomed.2009.11.012.

Hydrogen Peroxide is the Major Oxidant Product of Xanthine Oxidase

Eric E. Kelley[1,2], **Nicholas K.H. Khoo**[3], **Nicholas J. Hundley**[2], **Umair Z. Malik**[3], **Bruce A. Freeman**[3], and **Margaret M. Tarpey**[1,2,4]

[2]Department of Anesthesiology, University of Pittsburgh, School of Medicine

[3]Department of Pharmacology and Chemical Biology, University of Pittsburgh, School of Medicine

[4]Pittsburgh VA Medical Center

Abstract

Xanthine oxidase (XO) is a critical source of reactive oxygen species (ROS) in inflammatory disease. Focus, however, has centered almost exclusively on XO-derived superoxide ($O_2^{\bullet-}$) while direct H_2O_2 production from XO has been less well-investigated. Therefore, we examined the relative quantities of $O_2^{\bullet-}$ and H_2O_2 produced by XO under a range (1–21%) of O_2 tensions. At O_2 concentrations between 10 and 21 %, H_2O_2 accounted for ~ 75% of ROS production. As O_2 concentrations were lowered, there was a concentration-dependent increase in H_2O_2 formation, accounting for 90% of ROS production at 1% O_2. Alterations in pH between 5.5 and 7.4 did not affect the relative proportions of H_2O_2 and $O_2^{\bullet-}$ formation. Immobilization of XO, by binding to heparin-Sepharose, further enhanced relative H_2O_2 production by ~30%, under both normoxic and hypoxic conditions. Furthermore, XO bound to glycosaminoglycans (GAGs) on the apical surface of bovine aortic endothelial cells demonstrated a similar ROS production profile. These data establish H_2O_2 as the dominant (70–95%) reactive product produced by XO under clinically relevant conditions and emphasize the importance of H_2O_2 as a critical factor when examining the contributory roles of XO-catalyzed ROS in inflammatory processes as well as cellular signaling.

Introduction

The molybdoflavin enzyme, xanthine oxidoreductase (XOR) catalyzes the terminal two steps of purine degradation (hypoxanthine → xanthine → uric acid) in humans. XOR is transcribed as a single gene product, xanthine dehydrogenase (XDH). Substrate-derived electrons at the Mo-cofactor of XDH are transferred via Fe/S centers to a FAD moiety where NAD^+ is reduced to NADH. During inflammatory conditions, post-translational modification by oxidation of critical cysteine residues or limited proteolysis converts XDH to xanthine oxidase (XO) (1,2). The key difference between XDH and XO is the structural conformation and electrostatic microenvironment surrounding the FAD resulting in a decreased affinity for NAD^+ and enhancement of affinity for O_2 (3). Substrate-derived electrons at the Mo-cofactor of XO reduce O_2 at the FAD-cofactor both univalently, generating superoxide ($O_2^{\bullet-}$), and divalently,

1Address correspondence to: Eric E. Kelley, Ph.D., University of Pittsburgh, School of Medicine, Department of Anesthesiology, W-1357 Biomedical Sciences Tower, 200 Lothrop Street, Pittsburgh, PA, 15213, Phone: 412-648-9683, Fax: 412-648-9587, ekelley@pitt.edu, Margaret M. Tarpey, M.D., University of Pittsburgh, School of Medicine, Department of Anesthesiology, W-1358 Biomedical Sciences Tower, 200 Lothrop Street, Pittsburgh, PA, 15213, Phone: 412-648-9684, Fax: 412-648-9587, mtarpey+@pitt.edu .

forming hydrogen peroxide (H_2O_2). However, conversion to XO is not requisite for ROS production, as XDH displays partial oxidase activity under conditions in which NAD^+ levels are diminished such as the ischemic/hypoxic microenvironment encountered in vascular inflammation (4). This same inflammatory milieu leads to enhanced XO levels and thus increased XO-derived ROS formation resulting in activation of redox-dependent cell signaling reactions and alterations in vascular function. Evidence of this role for XO is exemplified by numerous studies in which XO inhibition attenuates symptoms of vascular disease including congestive heart failure, sickle cell anemia and diabetes (5–8).

Reports of XO-derived ROS production frequently address XO as the $O_2^{\bullet-}$-producing form of XDH and H_2O_2 is produced as a secondary byproduct of spontaneous or enzymatic dismutation of $O_2^{\bullet-}$. A crucial concept is often overlooked, specifically, that under relatively physiologic conditions (21% O_2 and pH 7.0) XO catalyzes the reduction of O_2 to H_2O_2 and $O_2^{\bullet-}$ at a ratio of 4:1 (H_2O_2:$O_2^{\bullet-}$) or ~80% H_2O_2 and ~20% $O_2^{\bullet-}$, whereas production of 100% $O_2^{\bullet-}$ requires an environment of 100% O_2 at pH 10 (9). While some studies have acknowledged this characteristic of XO (10–15), it is vastly underappreciated in the literature where focus remains fixed on $O_2^{\bullet-}$ as the key reactive product derived from XO. In addition, a limited number of biochemical studies addressing XO-mediated H_2O_2 production have centered on hyperoxia and/or alkaline conditions, which are less reflective of pathophysiologic conditions under which XOR most likely exerts significant influences (9,16–18). With renewed attention being focused on XO-derived ROS in numerous inflammatory processes, the relationship between O_2 concentration and XO-catalyzed $H_2O_2/O_2^{\bullet-}$ formation is crucial for the evaluation of contributory roles of XO and subsequent design of pharmacological approaches for treatment. *In toto*, these issues affirm the need for the examination of XO-derived ROS under clinically relevant conditions as performed herein.

Materials and Methods

Materials

Xanthine, allopurinol, diphenyleneiodonium chloride (DPI), Chelex resin, catalase and uric acid were from Sigma (St. Louis, MO). Medium 199 and fetal bovine serum (FBS) were from Invitrogen (Carlsbad, CA). Superoxide dismutase (CuZnSOD) was from OXIS International Inc. (Portland, OR).

Buffer Treatment

Buffers for all experiments were prepared from MilliQ H_2O and treated with Chelex resin to remove adventitious metals and thus minimize loss of ROS by metal-catalyzed reactions.

XO Activity

Enzyme was purified from fresh bovine cream by the method of Rajagopalan and stored in ammonium sulfate at 4°C until immediately before use (19). Enzymatic activity was determined either spectrophotometrically by the rate of uric acid formation monitored at 292 nm in 50 mM potassium phosphate (KPi), pH 7.4 ($\varepsilon = 11\ mM^{-1}\ cm^{-1}$) or electrochemically via reverse phase HPLC analysis of uric acid production (ESA CoulArray System, Chelmsford, MA), (1 Unit = 1 μmole urate/min) as previously (20). XDH activity was distinguished from XO activity by incubation with NAD^+ as previously described (21). Formation of $O_2^{\bullet-}$ was assessed by the SOD-inhibitable reduction of cytochrome c (550 nm) (9).

Univalent/Divalent Flux

Univalent flux was determined as previously reported (9). Briefly, under saturating xanthine concentrations, the total electron flux through the enzyme to O_2 was calculated as the rate of

uric acid formation. Under saturating cytochrome *c* concentrations, the rate of SOD-inhibitable cytochrome *c* reduction represents a measure of electron flux via the univalent reduction of O_2 to $O_2^{\bullet -}$. Dividing the cytochrome c reduction rate (1 e^-) by the uric acid formation rate (2 e^-) gives the % univalent flux (cyto *c* / 2(uric acid) ×100). As O_2 is the sole oxidizing substrate in the system, the divalent flux is derived by subtracting % univalent flux from 100.

XO Binding to GAGs

Xanthine oxidase was bound to heparin Sepharose 6B (HS6B) as previously (20). Briefly, XO (2 mg/ml) was added to a fixed amount of gel (0.05 g dry weight) and the mixture gently stirred in 5 mM KPi, pH 7.4 (2 ml final volume) at 25°C for 30 min. The suspension was centrifuged at 10,000 × g for 5 min, washed and the pellet resuspended in 5 mM KPi, pH 7.4. A quantity of HS6B-XO, equaling 5 mU/ml of XO activity, was added to PBS pH 7.4 in a 3 ml cuvette containing a small stir bar. Continuous gentle stirring was maintained with a Helma electronic stirrer placed inside the spectrophotometer cavity.

Oxygen Tension Experiments

Experiments at specific oxygen tensions were performed in a table-top glove box (Coy Instruments, Grass Lake, MI, USA) purged with N_2. All buffers were equilibrated >18 h before use. Glove box atmospheric O_2 conditions were followed with an O_2 monitor (Maxtec, Salt Lake City, UT) and O_2 concentrations verified with a clinical blood gas analyzer. Spectrophotometric determinations were carried out in gas tight cuvettes. Real time concentrations of molecular O_2 were determined polarographically using an Apollo 4000 Free Radical Analyzer (World Precision Instruments, Sarasota, FL, USA). Experiments were performed at standard temperature (25°C) and pressure (1 Atm).

Cellular Studies

Bovine aortic endothelial cells (BAEC) were isolated as previously (22). Primary cell culture, routine passage and experimental manipulations were all conducted in the absence of proteases. Cells were propagated by sub-culturing (1:4 ratios) in Medium 199 containing 5% FBS and thymidine (10 μM). Cells were utilized between passages 4 and 8 and were monitored visually for typical cobblestone morphology indicative of endothelial cells and by staining for von Willebrand factor expression. For O_2 consumption studies, confluent BAEC were exposed to XO (5 mU/ml) for 20 min at 25°C, harvested by mechanical dissociation, washed thoroughly (3 times with ice-cold PBS, pH 7.4), resuspended as a single-cell suspension (2×10^6 cells / ml) and placed on ice (for less than 1 h) until warmed to 25°C immediately before evaluation. This method minimizes cellular internalization of the enzyme as we have previously demonstrated (23). Cell viability was 93% following 1 h on ice as determined by Trypan blue dye exclusion. Oxygen consumption studies were performed under various O_2 tensions, as above, in the presence and absence of 50 U/ml CAT and/or SOD.

Statistics

Data were analyzed using one way analysis of variance followed by Tukey's range test for multiple pair-wise comparisons. Significance was determined as $p < 0.05$.

Results

Univalent/Divalent Flux

At 21% O_2, oxidation of xanthine (100 μM) to uric acid by XO (5 mU/ml) resulted in 28.1 ± 1.4% univalent flux ($O_2^{\bullet -}$ formation) in accordance with our previous reports, Table 1 (20, 24). Between 21 and 5% O_2, univalent flux remained relatively constant at ~70 %. As O_2 concentration was lowered below 5%, there was an O_2-dependent decrease in univalent flux

so that $O_2^{\bullet-}$ formation accounted for only 10% of electron flow through the enzyme at 1% O_2. Likewise, XO-dependent divalent reduction of O_2 to H_2O_2 increased from 72 % (21% O_2) to 90% (1% O_2). As O_2 tensions dropped below the K_m for O_2 (46 μM) an O_2-dependent decrease in the total electron flux (as determined by the formation of uric acid) through the enzyme was observed (1% = 13 μmoles/min, 2.5% = 18 μmoles/min and 5% = 2.3 μmoles/min) (1, 2.5 and 5% O_2 = ~13, 29 and 59 μM O_2, respectively) (25). This was reflected by a decrease in the overall rates of both uric acid formation and cytochrome *c* reduction. Control experiments conducted in the presence of catalase (CAT) demonstrated no H_2O_2-mediated reoxidation of cytochrome *c* during the initial 60 s of the reaction (the time frame for all univalent flux studies herein) that could account for the observed reduction in $O_2^{\bullet-}$ formation. Additional control experiments demonstrated that XO preparations were not contaminated with SOD as determined by both western-blot and activity assays. When O_2 tension was elevated to 95%, the percent univalent flux increased to 47.2 ± 2.3 (data not shown).

Oxygen Consumption

Initiation of XO turnover by addition of xanthine (100 μM), at 1% O_2, resulted in a rapid rate of O_2 consumption, Fig 1A. Increasing the O_2 concentration from 1–5% resulted in an O_2-dependent increase in the rate of O_2 consumption similar to the effects observed for univalent flux studies. At 1% O_2, the addition of CAT (50 U/ml) after 4.7 μM of O_2 was consumed, produced an immediate and pronounced evolution of O_2 (2.1 μM) from Reaction 1, Fig. 1B. Similar experiments carried out at different O_2 concentrations revealed an O_2-dependent diminution of CAT-induced O_2 evolution between 1–5% O_2 with no further decrease in O_2 evolved above 5% O_2, Fig. 1C and 1D. It is important to note that the quantity of H_2O_2 consumed by CAT is represented by 2 × O_2 evolved from Reaction 1. For example, at 1% O_2, CAT addition resulted in 2.1 μM O_2 evolution representing the enzymatic catalysis of 4.2 μM H_2O_2 and thus 89% of the O_2 consumed was due to H_2O_2 formation. Similar calculations for % H_2O_2 formation from O_2 consumption at the various O_2 tensions yielded: (89% (1% O_2), 77% (2.5% O_2), 72% (5% O_2), 64% (10% O_2), 68% (15% O_2) and 65% (21% O_2)).

$$2H_2O_2 \rightarrow 2H_2O + \mathbf{O_2} \qquad \text{Reaction 1}$$

$$O_2^{\bullet-} + O_2^{\bullet-} \rightarrow H_2O_2 + \mathbf{O_2} \qquad \text{Reaction 2}$$

Addition of SOD (50 mU/ml) during enzyme turnover did not alter the rate of O_2 consumption from Reaction 2, Fig. 2A. At 1% O_2, when SOD or CAT was added to the sample before xanthine, CAT significantly decreased the rate of O_2 consumption while SOD did not, Fig. 2B. However, the addition of both SOD and CAT resulted in an additional decrease in the O_2 consumption rate, compared to that produced by CAT alone, as diagrammed in Fig. 2C. Plotting the O_2 consumption rates in the presence of (SOD + CAT) as a percentage of the CAT only rates for each O_2 tension revealed an O_2-dependent decrease in the SOD + CAT rates from 1–5% O_2, Fig. 2D. For all O_2 consumption studies, addition of boiled CAT or SOD did not affect O_2 evolution or rates of O_2 consumption, not shown.

Effects of pH

The effect of pH (5.5–7.4) on the relative proportions of $O_2^{\bullet-}$ and H_2O_2 formation by XO were determined under various O_2 concentrations (1–21%) at saturating xanthine concentrations (100 μM). There was no effect of pH on univalent/divalent flux at any of the O_2 concentrations examined, data not shown.

XO-Immobilization

At 21% O_2, immobilization of XO by binding to heparin-Sepharose 6B (HS6B-XO) reduced the rates of urate formation and cytochrome *c* reduction as we reported previously (20), Table 2 and online supplement. In addition to an immobilization-induced reduction of total electron flow through the enzyme, the relative proportion of $O_2^{\bullet-}$ and H_2O_2 was also altered, reducing univalent electron transfer to O_2 by 30% compared to XO in solution. This immobilization-induced reduction in univalent flux was consistent for all O_2 tensions examined, such that at 1% O_2, univalent flux was only 6.9 % for bound XO compared to 10.4% univalent flux for free XO.

Endothelial cell-bound XO

Xanthine oxidase was bound to extracellular GAGs on the apical surface of BAEC as described in the methods. Cellular O_2 consumption studies were performed at various O_2 tensions (1–21%) in which CAT (200 U/ml), SOD (200 U/ml) or both were present before addition of xanthine. The effect of the presence of the antioxidants on the rate of XO-dependent O_2 consumption was determined and plotted as percent decrease when compared to control rates (no SOD or CAT) at each O_2 tension, Fig. 3. The presence of CAT significantly decreased the rate of O_2 consumption at all O_2 tensions resulting in a 27% decrease at 1% O_2 while SOD produced small, but significant, decreases (>5%) at O_2 levels above 2.5%. The presence of both SOD and CAT did not significantly alter rates of O_2 consumption compared to samples containing only CAT. Rates of O_2 consumption in the absence of xanthine were determined and subtracted from all values reported. When XO-treated cells were washed and then exposed to trypsin (0.25%) for 3 min at 37°C to remove/inactivate GAG-associated enzyme, no O_2 consumption was observed upon addition of xanthine demonstrating that ROS formation was from cell-associated XO. Furthermore, treatment with the XO-specific inhibitor, Febuxostat (25 μM), before addition of xanthine, abolished XO-dependent O_2 consumption, not shown.

Discussion

Studies on reactive species derived from XO have confirmed the biological production of $O_2^{\bullet-}$ (26). However, under normoxic conditions at neutral pH, XO produces significantly greater quantities of H_2O_2 (9). Perhaps of more significance, is that under the lower O_2 tensions and pH encountered during inflammation or ischemia, H_2O_2 accounts for 90–95% of XO-derived ROS formation, Table 1 and Table 2. These data confirm an O_2 dependence for ROS formation where lower O_2 concentrations lead to even greater H_2O_2 formation by XO. Conceptually, this can be illustrated by consideration of the overall oxidation/reduction state of the enzyme, Fig. 4. This scheme, albeit a very simplified representation of a complex series of electronic interactions between cofactors, summarizes the concept that a more reduced XO favors H_2O_2 production while a more oxidized XO favors $O_2^{\bullet-}$ formation. This effect of the redox state of XO on H_2O_2 vs. $O_2^{\bullet-}$ production has been previous reported with purified enzyme at pH 8.5 and confirms that high concentrations of xanthine and low O_2 tensions result in greater H_2O_2 production while low concentrations of xanthine and high O_2 tensions result in greater $O_2^{\bullet-}$ formation (18,27–29). This is critical to note as hypoxia/inflammation leads to lower O_2 tensions, increased XO expression as well as increased hypoxanthine/xanthine levels from ATP catabolism and thus sets the stage for enhance vascular H_2O_2 production. Therefore, recognizing that both reducing substrate concentration and O_2 tension are the key factors determining the identity XO-mediated ROS formation, we examined the effects of O_2 tension in the presence of a saturating xanthine concentration (100 μM). We chose this xanthine level as it reflects the concentrations encountered *in vivo* under ischemic/hypoxic conditions where ATP breakdown results in elevation of hypoxanthine/xanthine levels from ~2 μM to 50–100 μM, well above its K_m (6.5 μM) (20). In aggregate, our studies were designed to confirm and

expand the observations of previous studies under clinically-relevant conditions and to refocus attention on XO-derived H_2O_2.

Electron flux studies utilize uric acid formation and cytochrome *c* reduction to determine univalent flux; however, they do not directly measure divalent flux and thus it is a derived value. In a simple system in which O_2 is the sole electron acceptor, this is a valid calculation; however, an alternative approach which measures XO-derived H_2O_2 formation would confirm conclusions based on this derivation. Oxygen consumption was chosen to examine XO-dependent H_2O_2 formation in the presence and absence of CAT and SOD, the enzymes most often used to substantiate contributions of H_2O_2 and $O_2^{\bullet-}$ in biological systems, Fig. 1. This avoids possible direct interactions with XOR, ROS specificity issues and the potential of redox cycling which limit the specificity and sensitivity of several dye-based H_2O_2 assays (30). At 1% O_2, CAT addition resulted in significant evolution of O_2, indicating that 89% of the O_2 consumed by XO was reduced to H_2O_2. Values obtained at other O_2 tensions were also similar to, yet slightly lower than, the divalent fluxes listed in Table 1 supporting the validity of this approach. Lower yields for the O_2 evolution experiments may be due to the extended time (~2 min) of enzyme turnover and thus potential loss of H_2O_2 before the addition of CAT and/or subtle variations in temperature and barometric pressure.

Since CAT addition experiments confirmed the proportion of H_2O_2 formed during XO-catalyzed O_2 consumption, then the remainder of O_2 consumption should be attributable to $O_2^{\bullet-}$ formation. However, at 1% O_2, the presence of SOD before or after (Fig. 2) the addition of xanthine resulted in neither O_2 evolution nor alteration of the O_2 consumption rate. It is hypothesized that loss of $O_2^{\bullet-}$ from spontaneous dismutation (~2×10^5 M^{-1} s^{-1}), reaction with protein in the sample and degree of assay sensitivity all contributed to the absence of observable effects. To further address this issue, experiments were performed in which both SOD and CAT were present before initiation of enzyme turnover. At all O_2 tensions, addition of SOD + CAT before xanthine decreased the rate of O_2 consumption compared to samples containing only CAT, Fig. 2C and 2D. It is assumed that both O_2 evolution and the formation of additional CAT substrate (H_2O_2) by SOD (Reaction 2) served to augment total O_2 evolution. The CAT + SOD-induced decreases in O_2 consumption rates were not O_2-dependent above 5% O_2 (Fig. 2D) which is consistent with data from univalent flux studies showing no significant increase in $O_2^{\bullet-}$ formation from 5–21% O_2. This result is also consistent with the argument that as O_2 levels exceed the K_m of O_2 with the FAD (46 μM), a constant rate of $O_2^{\bullet-}$ formation would ensue where the presence of SOD offers no additional contribution to O_2 evolution and subsequent reduction in the rate of O_2 consumption in this O_2 concentration range (46–235 μM or 5–21%).

Inflammation is often characterized by both hypoxia and lowered pH; thus, it is important to consider the effects of H^+ ion concentration on ROS production by XO. The oxidation of xanthine at the Mo-cofactor is base-catalyzed and thus sensitive to changes of pH in the physiological range as well as substrate concentration (27). However, under saturating xanthine concentrations, the relative proportion of H_2O_2 to $O_2^{\bullet-}$ at each O_2 tension examined was not altered by pH (5.5–7.4).

During inflammatory conditions XDH is released into the circulation, rapidly converted to XO and avidly binds (K_d = 6 nM) to negatively charged glycosaminoglycans (GAGs) on the surface of vascular endothelial cells (24,31–33). This sequestration of XO by GAGs substantially amplifies local enzyme concentration, diminishes its rotational and translational mobility, thus, altering kinetic properties and conferring resistance to both product-induced and pharmacological inhibition (20,24). GAG association of XO decreases substrate binding affinity and thus increases the K_m for xanthine (6.5 μM *free* vs. 21.2 μM *bound*) and K_i for oxypurinol (85 nM *free* vs. 451 nM *bound*) when compared to XO in solution (24,34). These

characteristics indicate that XO bound to endothelial cell GAGs could serve as a long-lived source of ROS in this microenvironment. It is in this setting that XO-generated ROS can critically impact vessel function, emphasizing the need to more clearly define the effects of O_2 tension on ROS production by GAG-bound XO. Our previous studies demonstrate immobilization of XO on heparin-Sepharose reduces univalent flux by 30% in room air (20). At every O_2 concentration examined, GAG immobilization of XO produced a similar ~30% reduction in univalent flux, so that at 1% O_2, 93% of the ROS formed was H_2O_2. These data suggest XO-derived ROS production is almost exclusively H_2O_2 when XO is bound to endothelial GAGs in a hypoxic vascular milieu. To test this hypothesis in a cellular model, BAEC were exposed to purified XO and XO-dependent O_2 consumption was monitored over time in the presence of SOD, CAT or CAT + SOD, Fig. 3. The presence of SOD slightly altered O_2 consumption rates only when O_2 tensions exceeded 5%. In contrast, CAT significantly decreased rates of O_2 consumption as XO-produced H_2O_2 was converted to H_2O and O_2. These CAT-dependent decrements in O_2 consumption rates were seen at all O_2 tensions, with the greatest effects observed below 5% where H_2O_2 production would be expected to account for a preponderance of total ROS formation. The presence of both CAT and SOD produced O_2 consumption rates that were not statistically different from rates produced by samples containing only CAT. While differences between the CAT + SOD and CAT only values did not demonstrate statistical significance, the individual mean values for CAT + SOD from 5–21% O_2 were all greater than the corresponding CAT only values, possibly suggesting contributions from SOD near the limit of detection. Combined, these data demonstrate that quantification and characterization of ROS from these cellular studies is problematic due to loss of both H_2O_2 and $O_2^{\bullet -}$ before reaction with CAT and SOD from many mechanisms including reactions with cellular constituents such as GSH. However, they do reveal similar trends to those observed in the biochemical studies and qualitatively demonstrate that H_2O_2 is the major ROS product of XO, especially at O_2 tensions relevant to vascular pathology.

Over the past several years, there is renewed interest in the role of XO in vascular inflammation as the number of studies demonstrating salutary effects of XO inhibition accumulate. In order to successfully evaluate the contribution of XO in these and future studies, it is crucial to understand the identity and relative proportions of the ROS produced by this complex enzyme under conditions reflective of the microenvironment in which they are formed. Herein, we revisit the underappreciated detail that H_2O_2 is the major (~75%) ROS produced by XO under normal aerobic conditions and expand this observation to demonstrate that under pathophysiologic conditions XO-derived H_2O_2 formation approaches 95%. These results affirm the need to more critically evaluate the role of H_2O_2 in studies where XO-derived ROS have been proposed to play a contributory role. For example, many of the vessel studies in which XO-derived $O_2^{\bullet -}$ reduces NO-mediated vasodilatation were conducted using 95% O_2. This O_2 tension is significantly higher than O_2 levels experienced *in vivo*, and also serves to greatly enhance XO-derived $O_2^{\bullet -}$ formation and possibly lead to misconceptions regarding the role XO in this model. Furthermore, assigning a causative role for XO-derived $O_2^{\bullet -}$ based upon the beneficial actions of allopurinol administration, in the absence of controls for XO-derived H_2O_2, may result in neglecting pivotal signaling events mediated by H_2O_2, a molecule with an expanding number of targets in various cell signaling pathways (35–37).

Combined, the results from this report refocus attention on previous and commonly overlooked studies reporting H_2O_2 as the major ROS product of XO under normoxia. Furthermore, these data demonstrate that under pathophysiologic conditions XO-derived H_2O_2 formation approaches 95% and thus underscores the danger of failing to appreciate this attribute when investigating contributory roles for XO in pathology.

Abbreviations

BAEC	bovine aortic endothelial cells
CAT	catalase
GAGs	glycosaminoglycans
ROS	reactive oxygen species
SOD	superoxide dismutase
XDH	xanthine dehydrogenase
XO	xanthine oxidase
XOR	xanthine oxidoreductase

Acknowledgments

This study was supported by a University of Pittsburgh, Department of Anesthesiology Seed Grant (EEK). The authors would like to thank Dr. Joe S. Moritz, Ph.D. and Dr. Keith Inskeep, Ph.D., Division of Animal and Veterinary Science, West Virginia University, Morgantown, WV for both fresh cream and chicken livers used in enzyme purification.

References

1. Amaya Y, Yamazaki K, Sato M, Noda K, Nishino T. Proteolytic conversion of xanthine dehydrogenase from the NAD-dependent type to the O_2-dependent type. Amino acid sequence of rat liver xanthine dehydrogenase and identification of the cleavage sites of the enzyme protein during irreversible conversion by trypsin. J.Biol.Chem 1990;265:14170–14175. [PubMed: 2387845]
2. Waud WR, Rajagopalan KV. The mechanism of conversion of rat liver xanthine dehydrogenase from an NAD^+-dependent form (type D) to an O_2-dependent form (type O). Arch.Biochem.Biophys 1976;172:365–379. [PubMed: 176940]
3. Enroth C, Eger BT, Okamoto K, Nishino T, Nishino T, Pai EF. Crystal structures of bovine milk xanthine dehydrogenase and xanthine oxidase: Structure-based mechanism of conversion. Proc.Natl.Acad.Sci.USA 2000;97:10723–10728. [PubMed: 11005854]
4. Harris CM, Massey V. The Oxidative Half-reaction of Xanthine Dehydrogenase with NAD; Reaction Kinetics and Steady-state Mechanism. J.Biol.Chem 1997;272:28335–28341. [PubMed: 9353290]
5. Butler R, Morris AD, Belch JJ, Hill A, Struthers AD. Allopurinol normalizes endothelial dysfunction in type 2 diabetics with mild hypertension. Hypertension 2000;35:746–751. [PubMed: 10720589]
6. Desco MC, Asensi M, Marquez R, Martinez-Valls J, Vento M, Pallardo FV, Sastre J, Vina J. Xanthine oxidase is involved in free radical production in type 1 diabetes: protection by allopurinol. Diabetes 2002;51:1118–1124. [PubMed: 11916934]
7. Farquharson CA, Butler R, Hill A, Belch JJ, Struthers AD. Allopurinol improves endothelial dysfunction in chronic heart failure. Circulation 2002;106:221–226. [PubMed: 12105162]
8. Aslan M, Ryan TM, Adler B, Townes TM, Parks DA, Thompson JA, Tousson A, Gladwin MT, Patel RP, Tarpey MM, Batinic-Haberle I, White CR, Freeman BA. Oxygen radical inhibition of nitric oxide-dependent vascular function in sickle cell disease. Proc.Natl.Acad.Sci.USA 2001;98:15215–15220. [PubMed: 11752464]
9. Fridovich I. Quantitative aspects of the production of superoxide anion radical by milk xanthine oxidase. J.Biol.Chem 1970;245:4053–4057. [PubMed: 5496991]
10. McCutchan HJ, Schwappach JR, Enquist EG, Walden DL, Terada LS, Reiss OK, Leff JA, Repine JE. Xanthine oxidase-derived H_2O_2 contributes to reperfusion injury of ischemic skeletal muscle. Am.J.Physiol 1990;258:H1415–H1419. [PubMed: 2110780]
11. Brown JM, Terada LS, Grosso MA, Whitmann GJ, Velasco SE, Patt A, Harken AH, Repine JE. Xanthine oxidase produces hydrogen peroxide which contributes to reperfusion injury of ischemic, isolated, perfused rat hearts. J.Clin.Invest 1988;81:1297–1301. [PubMed: 3127425]

12. Siems W, Schmidt H, Muller M, Henke W, Gerber G. H_2O_2 formation during nucleotide degradation in the hypoxic rat liver: a quantitative approach. Free Radic.Res.Commun 1986;1:289–295. [PubMed: 2850267]
13. Patt A, Harken AH, Burton LK, Rodell TC, Piermattei D, Schorr WJ, Parker NB, Berger EM, Horesh IR, Terada LS. Xanthine oxidase-derived hydrogen peroxide contributes to ischemia reperfusion-induced edema in gerbil brains. J.Clin.Invest 1988;81:1556–1562. [PubMed: 3130395]
14. Fatokun AA, Stone TW, Smith RA. Hydrogen peroxide mediates damage by xanthine and xanthine oxidase in cerebellar granule neuronal cultures. Neurosci.Lett 2007;416:34–38. [PubMed: 17360118]
15. Lee H, Carlson JD, McMahon KK, Moyer TP, Fischer AG. Xanthine oxidase: a source of hydrogen peroxide in bovine thyroid glands. Life Sci 1977;20:453–458. [PubMed: 14288]
16. Lacy F, Gough DA, Schmid-Schonbein GW. Role of xanthine oxidase in hydrogen peroxide production. Free Radic.Biol.Med 1998;25:720–727. [PubMed: 9801073]
17. Kellogg EW III, Fridovich I. Superoxide, hydrogen peroxide, and singlet oxygen in lipid peroxidation by a xanthine oxidase system. J.Biol.Chem 1975;250:8812–8817. [PubMed: 171266]
18. Porras AG, Olson JS, Palmer G. The reaction of reduced xanthine oxidase with oxygen. Kinetics of peroxide and superoxide formation. J.Biol.Chem 1981;256:9006–9103. [PubMed: 6267059]
19. Waud WR, Brady FO, Wiley RD, Rajagopalan KV. A new purification procedure for bovine milk xanthine oxidase: effect of proteolysis on the subunit structure. Arch. Biochem. Biophys 1975;169:695–701. [PubMed: 1180567]
20. Kelley EE, Trostchansky A, Rubbo H, Freeman BA, Radi R, Tarpey MM. Binding of Xanthine Oxidase to Glycosaminoglycans Limits Inhibition by Oxypurinol. J.Biol.Chem 2004;279:37231–37234. [PubMed: 15231841]
21. Suzuki H, DeLano FA, Parks DA, Jamshidi N, Granger DN, Ishii H, Suematsu M, Zweifach BW, Schmid-Schonbein GW. Xanthine oxidase activity associated with arterial blood pressure in spontaneously hypertensive rats. Proc.Natl.Acad.Sci.USA 1998;95:4754–4759. [PubMed: 9539811]
22. Kelley EE, Hock T, Khoo NKH, Richardson GR, Johnson KK, Powell PC, Giles GI, Agarwal A, Lancaster JR Jr, Tarpey MM. Moderate hypoxia induces xanthine oxidoreductase activity in arterial endothelial cells. Free Radic.Biol.Med 2006;40:952–959. [PubMed: 16540390]
23. Kelley EE, Batthyany CI, Hundley NJ, Woodcock SR, Bonacci G, Del Rio JM, Schopfer FJ, Lancaster JR Jr, Freeman BA, Tarpey MM. Nitro-oleic Acid, a Novel and Irreversible Inhibitor of Xanthine Oxidoreductase. J.Biol.Chem 2008;283:36176–36184. [PubMed: 18974051]
24. Radi R, Rubbo H, Bush K, Freeman BA. Xanthine oxidase binding to glycosaminoglycans: kinetics and superoxide dismutase interactions of immobilized xanthine oxidase-heparin complexes. Arch.Biochem.Biophys 1997;339:125–135. [PubMed: 9056242]
25. Saito T, Nishino T. Differences in redox and kinetic properties between NAD-dependent and O_2-dependent types of rat liver xanthine dehydrogenase. J.Biol.Chem 1989;264:10015–10022. [PubMed: 2722858]
26. McCord JM, Fridovich I. The reduction of cytochrome c by milk xanthine oxidase. J.Biol.Chem 1968;243:5753–5760. [PubMed: 4972775]
27. Hille R, Massey V. Studies on the oxidative half-reaction of xanthine oxidase. J.Biol.Chem 1981;256:9090–9095. [PubMed: 6894924]
28. Olson JS, Ballow DP, Palmer G, Massey V. The reaction of xanthine oxidase with molecular oxygen. J.Biol.Chem 1974;249:4350–4362. [PubMed: 4367214]
29. Olson JS, Ballou DP, Palmer G, Massey V. The mechanism of action of xanthine oxidase. J.Biol.Chem 1974;249:4363–4382. [PubMed: 4367215]
30. Tarpey MM, Fridovich I. Methods of detection of vascular reactive species: nitric oxide, superoxide, hydrogen peroxide, and peroxynitrite. Circ.Res 2001;89:224–236. [PubMed: 11485972]
31. Adachi T, Fukushima T, Usami Y, Hirano K. Binding of human xanthine oxidase to sulphated glycosaminoglycans on the endothelial-cell surface. Biochem.J 1993;289:523–527. [PubMed: 8424793]
32. Fukushima T, Adachi T, Hirano K. The heparin-binding site of human xanthine oxidase. Biological & Pharmaceutical Bulletin 1995;18:156–158. [PubMed: 7735231]

33. Houston M, Estevez A, Chumley P, Aslan M, Marklund S, Parks DA, Freeman BA. Binding of xanthine oxidase to vascular endothelium. Kinetic characterization and oxidative impairment of nitric oxide-dependent signaling. J.Biol.Chem 1999;274:4985–4994. [PubMed: 9988743]

34. Camejo G, Olsson U, Hurt-Camejo E, Baharamian N, Bondjers G. The extracellular matrix on atherogenesis and diabetes-associated vascular disease. Atheroscler.Suppl 2002;3:3–9. [PubMed: 12044579]

35. Rhee SG, Kang SW, Jeong W, Chang TS, Yang KS, Woo HA. Intracellular messenger function of hydrogen peroxide and its regulation by peroxiredoxins. Curr.Opin.Cell Biol 2005;17:183–189. [PubMed: 15780595]

36. Forman HJ, Torres M. Reactive Oxygen Species and Cell Signaling: Respiratory Burst in Macrophage Signaling. Am.J.Respir.Crit.Care Med 2002;166:4S–8S.

37. Cai H. Hydrogen peroxide regulation of endothelial function: origins, mechanisms, and consequences. Cardiovasc.Res 2005;68:26–36. [PubMed: 16009356]

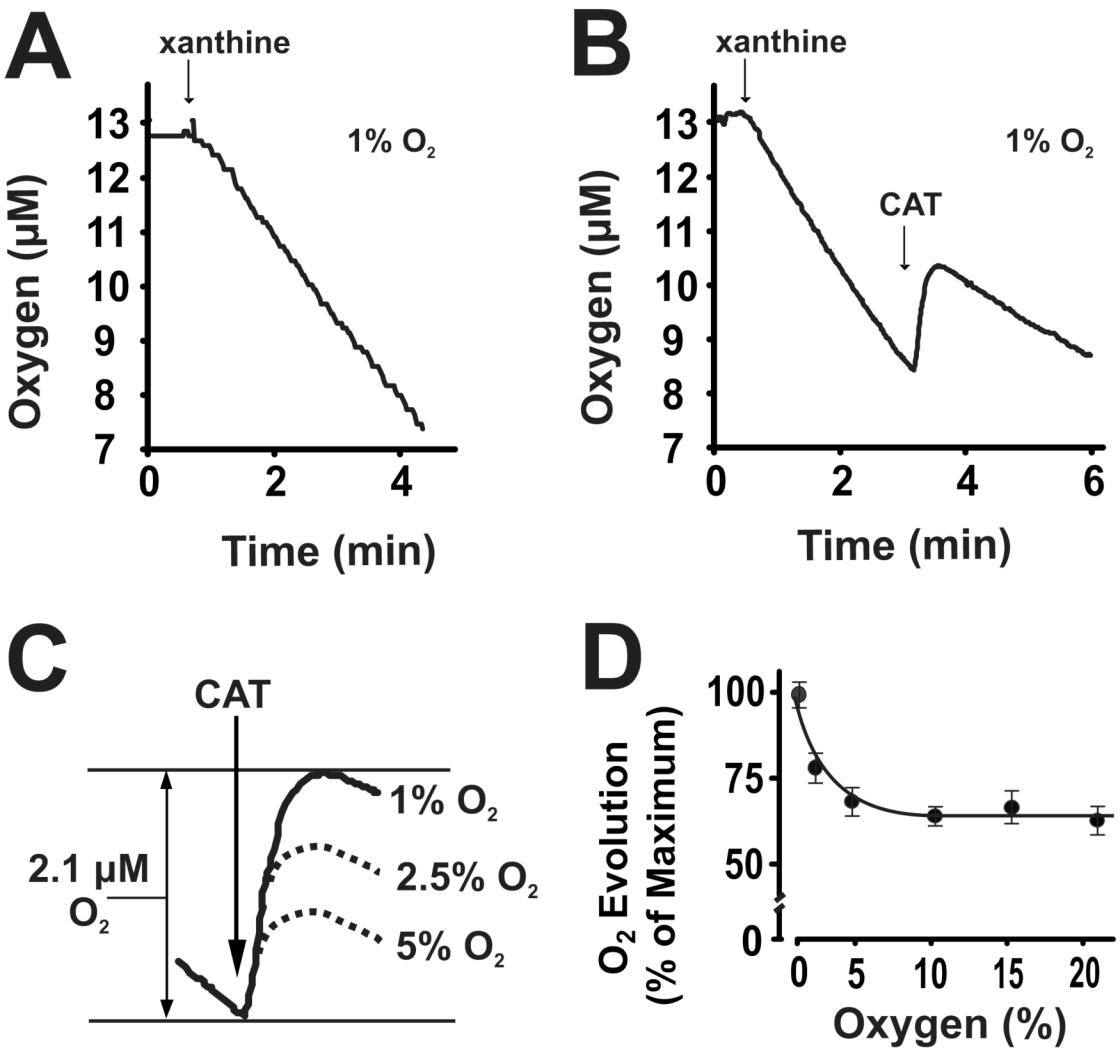

Fig. 1. H_2O_2 is the major ROS produced by XO at low O_2 tensions

(**A**) XO (20 mU/ml, PBS pH 7.2) was exposed to xanthine (100 μM) in a 1% O_2 atmosphere and O_2 concentration monitored polargraphically over time. (**B**) During the linear phase of O_2 consumption 50 U/ml catalase (CAT) ($2H_2O_2 \rightarrow 2H_2O + \mathbf{O_2}$) was added to the reaction. (**C**) Scheme showing total O_2 evolved (2.1 μM) by the addition of 50 U/ml CAT at 1% O_2 and the effect of increasing O_2 tension (1–5%) on the quantity of CAT-dependent O_2 evolution. (**D**) Using the quantity of O_2 evolved at 1% O_2 as maximum (100%), CAT-dependent O_2 evolution values are plotted as (% Maximum) for O_2 concentrations (1–21%). For each O_2 tension, CAT was added to the samples immediately after the same XO-dependent depletion of O_2 (4.7 μM). Values represent the mean of at least 4 independent determinations.

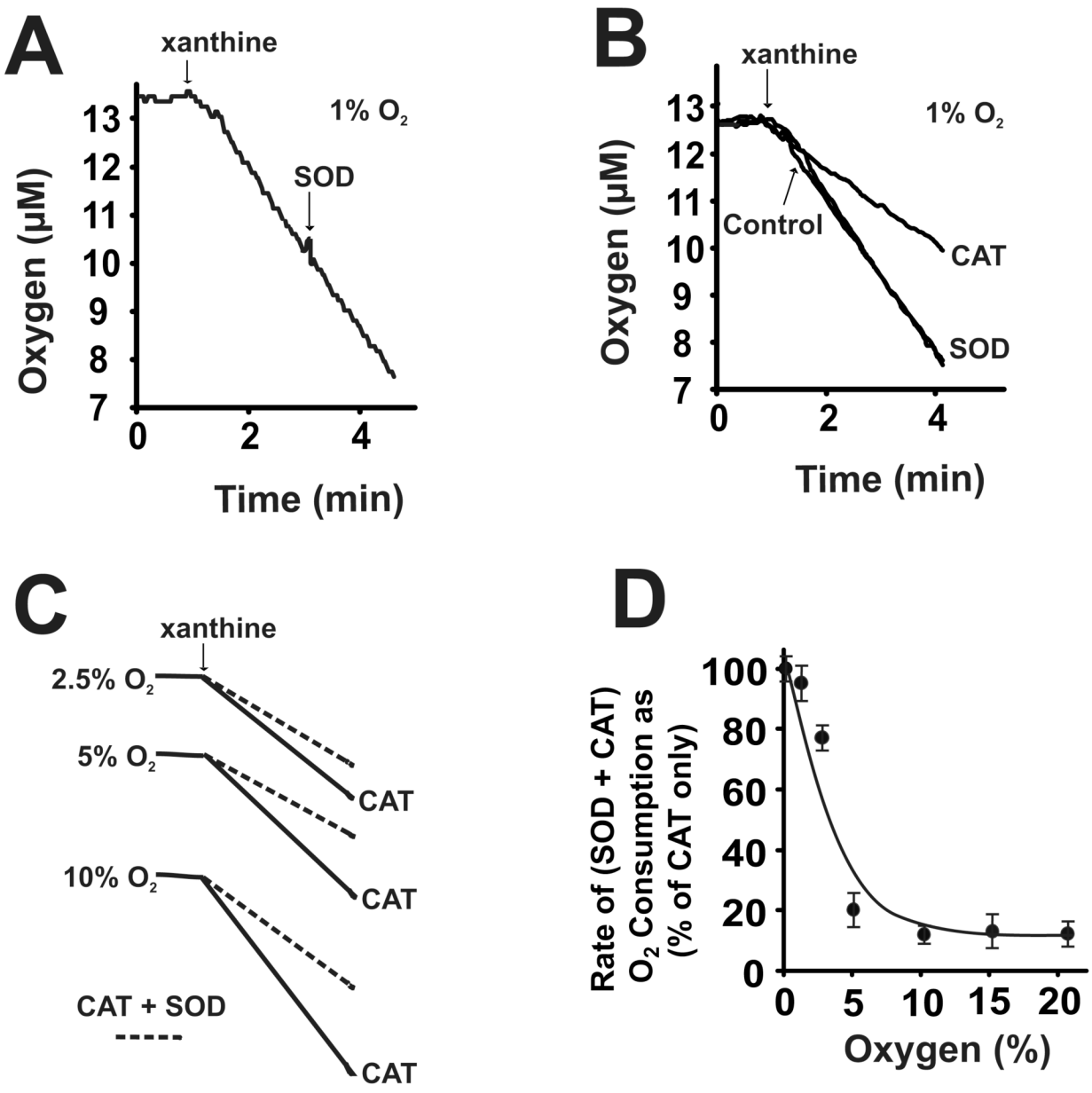

Fig. 2. Oxygen dependence of $O_2^{\bullet-}$ formation from XO

(**A**) XO (20 mU/ml, PBS pH 7.2) was exposed to xanthine (100 μM) at 1% O_2 as in Fig. 1. During the linear phase of O_2 consumption 50 U/ml SOD ($O_2^{\bullet-} + O_2^{\bullet-} \rightarrow H_2O_2 + \mathbf{O_2}$) was added to the reaction. (**B**) Either SOD or CAT were added to the sample before the initiation of enzyme turnover with xanthine (100 μM) and compared to control in the absence antioxidant. (**C**) Shown is a representative diagram of experiments conducted similar to those in B, but with SOD and CAT added together before xanthine. (**D**) The (SOD + CAT)-dependent decreases in the rate of O_2 consumption are plotted as percentage of the CAT only values (CAT only = 100%) at each O_2 concentration (1–21%). These (SOD + CAT)-dependent decreases in the rate of O_2 depletion result from evolution of O_2 from the following reactions: SOD ($O_2^{\bullet-} + O_2^{\bullet-} \rightarrow \mathbf{H_2O_2} + \mathbf{O_2}$) and CAT ($2H_2O_2 \rightarrow 2H_2O + \mathbf{O_2}$). Shown are representative experiments of at least 4 independent determinations.

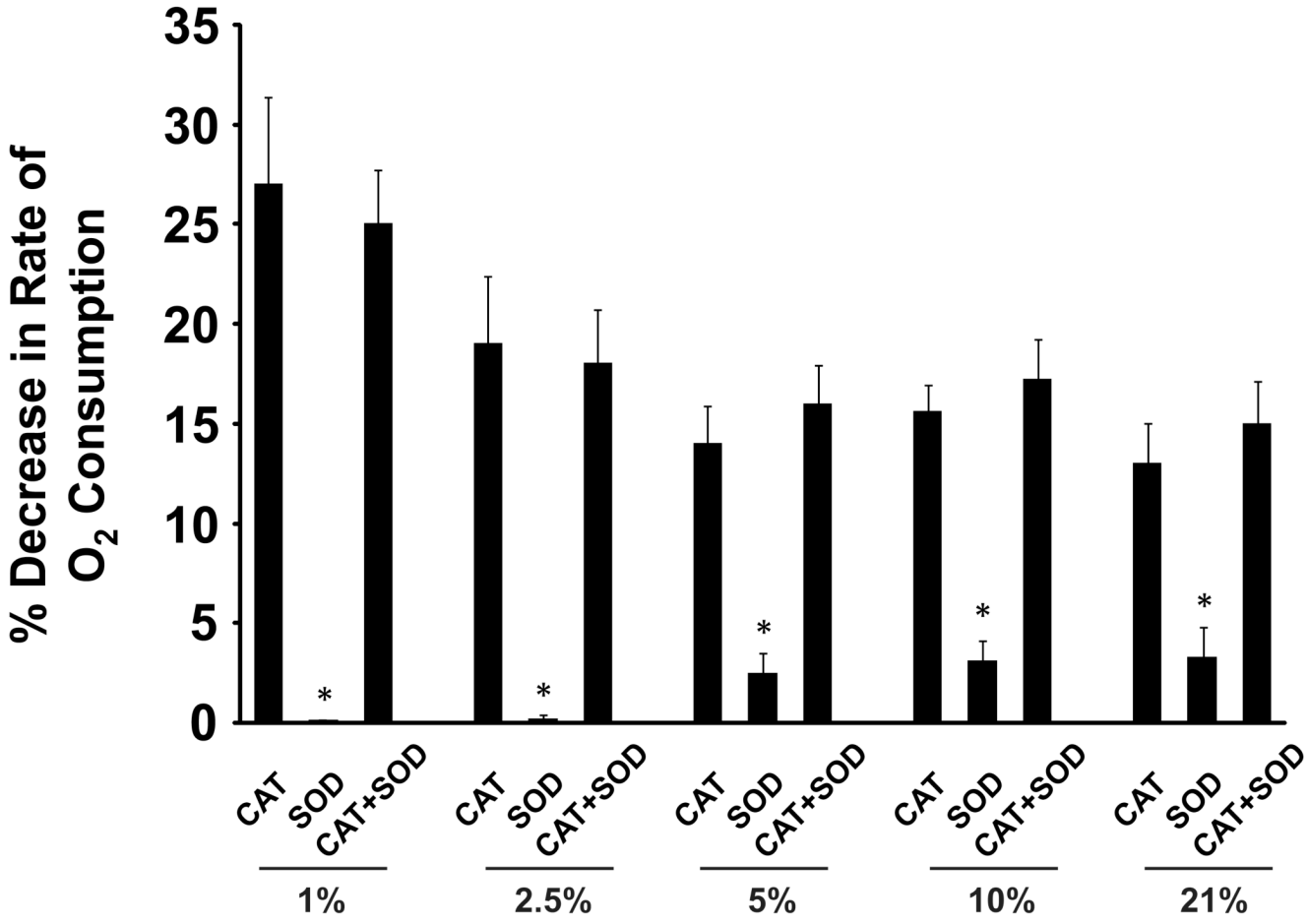

Fig. 3. H_2O_2 is the major ROS produced by endothelial cell-associated XO

BAEC were exposed to XO (5 mU/ml) as described in the methods. Cell suspensions (2×10^6 cells /ml) were monitored for O_2 consumption upon the addition of xanthine. Either SOD (200 U/ml), CAT (200 U/ml) or both were added to the samples before xanthine as indicated. The effects of the presence of (CAT, SOD, CAT+SOD) are represented as % decrease (***inset***) in the rate of O_2 consumption from control samples without antioxidant and are plotted for the indicated O_2 tensions. Values represent the mean of 3 independent determinations. (*) indicates $p < 0.05$ compared to CAT only and/or CAT+SOD.

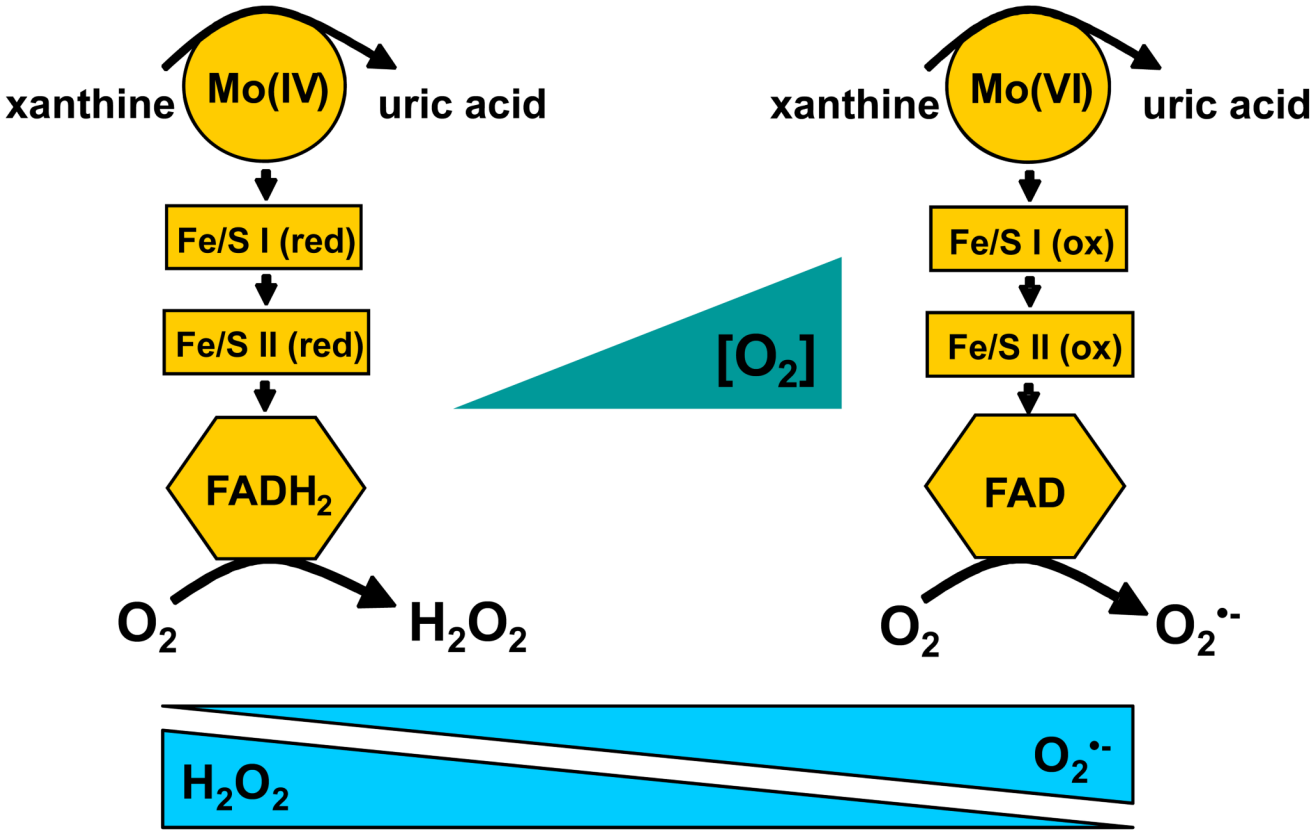

Fig. 4. Effects of O_2 on XO-derived ROS formation

Purine-derived electrons enter XO via the Mo-cofactor and egress through the FAD-cofactor by reaction with molecular O_2. Therefore, at physiological pH, the oxidation/reduction status of XO is dependent upon both the concentration of purine (xanthine/hypoxanthine) and O_2. Under saturating purine concentrations, O_2 tension is the prime determinant of this redox state of XO. Shown are 2 cartons depicting the extreme redox states (either fully oxidized or reduced) of the various co-factors in XO in the presence of saturating xanthine concentrations. On the left, under anoxia, the enzyme is fully reduced. Upon oxygenation, the reduced FAD-cofactor reacts with O_2 diavalently to produce H_2O_2. As O_2 levels increase so does O_2-mediated electron egress via the FAD-cofactor until it begins to out compete electron entry at the Mo-cofactor resulting in an increase in the overall oxidation of the enzyme. This increase in the oxidation of the enzyme shifts FAD-cofactor-O_2 reactions from divalent to univalent producing more $O_2^{\bullet -}$ and less H_2O_2.

Table 1
Oxygen dependence of univalent vs. divalent flux for XO

Purified XO (5 mU/ml) was exposed to xanthine (100 μM) and superoxide was measured by the SOD-inhibitable reduction of cytochrome *c* (λ = 550 nm). Divalent flux was derived by subtracting the percent univalent flux values from 100. Experiments were performed at standard temperature (25°C) and pressure (1 Atm).

$[O_2]$ %	$O_2^{\bullet-}$ *% Univalent Flux*	H_2O_2 *% Divalent Flux*
1	10.4 ± 0.6	90
2.5	14.3 ± 0.9	86
5	24.6 ± 2.3	76
10	28.5 ± 0.7	71
15	27.8 ± 0.5	72
21	28.1 ± 1.4	72

Values for univalent flux were calculated by monitoring the SOD-inhibitible reduction of cytochrome c (550 nm) as described in the methods. Values for divalent flux were derived by subtracting the percent univalent flux from 100.

Table 2
Oxygen dependence of univalent vs. divalent flux for GAG-imobilized XO

XO was immobilized on heparin-Sepharose 6B (HS6B-XO), exposed to xanthine (100 μM) and univalent flux ($O_2^{\bullet -}$ formation) determined by the SOD-inhibitable reduction of cytochrome *c* (λ = 550 nm) under the indicated O_2 tensions. Divalent flux (H_2O_2 formation) was derived by subtracting the percent univalent flux values from 100. Experiments were performed at standard temperature (25°C) and pressure (1 Atm).

$[O_2]$ %	% $O_2^{\bullet -}$		% H_2O_2	
	free	*bound*	*free*	*bound*
1	10.4 ± 0.6	6.9 ± 1.2	90	93
5	24.6 ± 2.3	17.4 ± 4.2	76	83
10	28.5 ± 0.7	18.9 ± 2.1	71	81
21	28.1 ± 1.4	19.8 ± 1.1	72	80

Values for univalent flux were calculated by monitoring the SOD-inhibitible reduction of cytochrome c (550 nm) as described in the methods. Values for divalent flux were derived by subtracting the percent univalent flux from 100.